

# Orthonormal Ladder Filters

D.A. Johns, W.M. Snelgrove, and A.S. Sedra

University of Toronto

## Abstract

A new state-space structure for the realization of arbitrary filter transfer-functions is presented. This structure should prove useful where integrators are the basic building blocks such as in transconductance-C, MOSFET-C, or active-RC filters. The structure is derived from a singly-terminated LC ladder and has the properties that it is always scaled for optimum dynamic range and its integrator outputs are orthogonal. For this reason, the resulting realizations are called "orthonormal ladder filters". Since dynamic range scaling is inherent to the proposed structure, it is felt that this design technique may be most useful in programmable or adaptive filters. Finally, the sensitivity and dynamic range properties of an orthonormal ladder filter are shown to be comparable in performance to the equivalent properties obtained from a cascade of biquads.

## 1. Introduction

When realizing high order transfer-functions, a circuit simulation of an LC ladder results in very good performance. The reason for this fact is the excellent passband sensitivity properties of doubly-terminated LC ladder filters [1]. However, passband sensitivity is not always the deciding factor in choosing a filter implementation. Other properties of a particular implementation may become important. For example, often a cascade

of biquads is implemented because of its ease of design, the ability to realize any stable transfer-function, or one of its many other features. This paper will introduce a new filter structure which has a sensitivity and dynamic range performance comparable to a cascade of biquads as well as other interesting and useful properties. We call the filters with this new structure “orthonormal ladder filters”.

Perhaps one of the more interesting properties of orthonormal ladder filters is the fact that the resulting circuits are inherently scaled for optimum dynamic range. Moreover, an  $L_2$  norm is used in dynamic range scaling as opposed to an  $L_\infty$  norm. Simply stated,  $L_2$  scaling implies that the output of each integrator will have the same RMS value when white noise is applied at the filter input. It is felt that this type of scaling covers a more general class of filters than  $L_\infty$  scaling where a swept sinusoid is applied at the input. Note that while  $L_2$  scaling is relatively difficult to apply to a cascade of biquads, the actual structure of orthonormal ladder filters ensures optimum dynamic range scaling with an  $L_2$  norm.

Another property of orthonormal ladder filters is the ability to realize any stable transfer-function. This is accomplished through the use of an output summing stage. Output summing is often avoided in practice because of fears of poor stopband sensitivity properties. However, through the use of two examples, it will be shown that an orthonormal ladder filter (including, of course, the output summing stage) has a sensitivity performance comparable to a good design of a cascade of biquads. Additionally, since for a given transfer-function the orthonormal ladder realization is unique, the design procedure is more easily automated than the process of finding an optimal biquad cascade design where pole-zero pairing and cascade ordering are important. It will also be shown that

the output summing stage can be replaced by using feed-forward to each of the inputs of the integrators.

Two other features of orthonormal ladder filters are: a close relationship to singly-terminated LC ladders, and uncorrelated integrator outputs when the filter input is white noise. The close relationship to singly-terminated ladders allows a simple synthesis procedure and a trivial stability check. Uncorrelated integrator outputs suggest the possibility of adaptive filtering with continuous-time signals.

Orthonormal filter structures are well known in the digital filter literature [2]. One of the reasons for their use is that overflow oscillations are impossible in these digital filters. However, their main disadvantage is that their structure is fairly dense. Fortunately, the structure for orthonormal ladder filters is quite sparse.

The state-space formulation is used to find and analyze the structure of the proposed orthonormal ladder filters. Section 2 defines the state-space description and the state correlation matrix, as well as deriving a formula which relates the state correlation matrix to the system matrices. Although this formula is well known in the control literature, it is derived here to emphasize its physical interpretation. When the state correlation matrix is the identity matrix, orthonormal systems are obtained. Orthonormal ladder synthesis is presented in section 3 where it is shown that singly-terminated ladders can be used to obtain orthonormal systems. An example of an orthonormal ladder design is presented in section 4. Section 5 presents a sensitivity and dynamic range comparison between orthonormal ladder filters, doubly-terminated LC ladder simulations and cascades of biquads. Finally, application areas for orthonormal ladder filters are suggested in section 6.

## 2. State-Space and the State Correlation Matrix

An  $N^{th}$  order state-space system can be described by the equations:

$$s\mathbf{X}(s) = \mathbf{A}\mathbf{X}(s) + \mathbf{b}U(s) \quad (1)$$

$$\mathbf{Y}(s) = \mathbf{c}^T \mathbf{X}(s) + dU(s)$$

where  $U(s)$  is the input signal;  $\mathbf{X}(s)$  is a vector of  $N$  states, which in fact are the integrator outputs;  $\mathbf{Y}(s)$  is the output signal; and  $\mathbf{A}$ ,  $\mathbf{b}$ ,  $\mathbf{c}$ , and  $d$  are coefficients relating these variables. The transfer-function of the above system is easily shown to be

$$T(s) = \mathbf{c}^T (s\mathbf{I} - \mathbf{A})^{-1} \mathbf{b} \quad (2)$$

As in [3], we define a vector of intermediate-functions,  $\mathbf{F}(s)$ , to be the transfer-functions from the filter input to the states,  $\mathbf{X}(s)$ . In the frequency domain<sup>1</sup>, the vector  $\mathbf{F}(s)$  is obtained from

$$\mathbf{F}(s) = (s\mathbf{I} - \mathbf{A})^{-1} \mathbf{b} \quad (3)$$

whereas in the time domain, the impulse response is given by

$$\mathbf{f}(r) = e^{\mathbf{A}r} \mathbf{b} \quad (4)$$

We require an inner product definition in order to find the correlation between the states of a given system and thus a correlation matrix,  $\mathbf{K}$ , such that  $K_{ij}$  is the inner product between  $F_i$  and  $F_j$ . Choosing to define the inner product as one which gives the squared  $L_2$  norms along the diagonal of  $\mathbf{K}$ , we have

$$K_{ij} = \langle F_i(s), F_j(s) \rangle = \int_{-\infty}^{\infty} F_i(j\omega) \overline{F_j(j\omega)} d\omega \quad (5)$$

---

<sup>1</sup>The variable  $\mathbf{F}$  in this paper corresponds to the variable  $\mathbf{f}$  in [3] (not the matrix  $\mathbf{F}$  in [3]). This change in notation is required to allow the representation of time-domain variables.

which equals the inner product in the time domain given by

$$\langle f_i(t), f_j(t) \rangle = 2\pi \int_0^{\infty} f_i(t) \bar{f}_j(t) dt \quad (6)$$

In the time domain, the matrix  $\mathbf{K}$  is found by combining equations (4) and (6).

$$\mathbf{K} = 2\pi \int_0^{\infty} e^{\mathbf{A}t} \mathbf{b} \mathbf{b}^T e^{\mathbf{A}^T t} dt \quad (7)$$

Differentiating the inside of the above integral, we find

$$\frac{d(e^{\mathbf{A}t} \mathbf{b} \mathbf{b}^T e^{\mathbf{A}^T t})}{dt} = \mathbf{A} e^{\mathbf{A}t} \mathbf{b} \mathbf{b}^T e^{\mathbf{A}^T t} + e^{\mathbf{A}t} \mathbf{b} \mathbf{b}^T e^{\mathbf{A}^T t} \mathbf{A}^T \quad (8)$$

and integrating both sides of equation (8) from 0 to  $\infty$ , the following Liapunov equation is obtained.

$$\mathbf{A} \mathbf{K} + \mathbf{K} \mathbf{A}^T + 2\pi \mathbf{b} \mathbf{b}^T = 0 \quad (9)$$

The above equation allows one to find the correlation matrix,  $\mathbf{K}$ , given the system matrices,  $\mathbf{A}$  and  $\mathbf{b}$ . Note that the the correlation matrix,  $\mathbf{K}$ , is called the controllability grammian in the control literature [4,5] and that a similar equation is obtained in the discrete- time domain [2].

Before leaving this section, we would like to describe another set of intermediate-functions. This second vector of functions,  $\mathbf{G}(s)$ , is defined to be the set of transfer functions from the input of the integrators to the output of the system. In the frequency domain,

$$\mathbf{G}(s) = \mathbf{c}^T (s\mathbf{I} - \mathbf{A})^{-1} \quad (10)$$

**This** set of functions,  $\mathbf{G}$ , together with the set of intermediate-functions  $\mathbf{F}$  allow simple analysis of sensitivity and dynamic range performance for a given state-space structure [3].



well, reactive components are labeled  $r_i$  where  $r_i$  is either the capacitor or inductor value. The matrices  $\mathbf{A}$  and  $\mathbf{b}$  of the state-space description of the ladder in figure 1 are found to be

$$\mathbf{A} = \begin{array}{c|cccccc} & 0 & \frac{1}{r_1} & & & & \mathbf{0} \\ & \frac{-1}{r_2} & 0 & \frac{1}{r_2} & & & \\ & & \frac{-1}{r_3} & 0 & \cdot & & \\ & & & \cdot & \cdot & & \\ & & & & \cdot & \mathbf{0} & \frac{1}{r_{N-1}} \\ & 0 & & & & -1 & -1 \\ & & & & & r_N & r_N \end{array} \quad \mathbf{b} = \begin{array}{c|c} & 0 \\ & 0 \\ & 0 \\ & \cdot \\ & 0 \\ & 1 \\ & r_N \end{array} \quad (12)$$

We can transform the above system to that of the orthonormal ladder system with the structure of equation (11) by an appropriate scaling of the system states. Scaling the  $i$ 'th state of a system by a factor  $\beta_i$  results in the  $i$ 'th row of  $\mathbf{A}$  and  $\mathbf{b}$  being multiplied by  $\beta_i$  and the  $i$ 'th column of  $\mathbf{A}$  divided by  $\beta_i$ . Using this fact, the required scaling factors,  $\beta_i$ , are found to be

$$\beta_i = \left\{ \frac{r_i}{\pi} \right\} \frac{r_i}{\pi} \frac{1}{2} \quad (13)$$

It should be noted that this scaling process does not change the system poles. Scaling the state-space description of equation (12) and comparing the result to the system in **(1 1)**, we find the following relationship between the elements of the orthonormal ladder system and the reactive components of the LC ladder:

$$\alpha_i = \left[ \frac{1}{r_i r_{i+1}} \right]^{\frac{1}{2}} \quad 1 \leq i < N \quad (14)$$

$$\alpha_N = \frac{1}{r_N}$$

1

Recall that our goal is to be able to place the poles of the orthonormal ladder system at given locations in the left-half  $s$ -plane. This can be accomplished by obtaining a singly-terminated LC ladder with the desired poles and then using the above equation to obtain the elements of the orthonormal system. From circuit theory, we know that any stable natural mode polynomial can be uniquely realized by an all-pole singly-terminated ladder with positive elements [6]. Thus, one can always find a unique orthonormal ladder system for any set of stable poles.

Note that an interesting property of all-pole singly-terminated LC ladders has become apparent. We have shown that the states (inductor currents and capacitor voltages) of an all-pole singly-terminated LC ladder are all orthogonal since the states in equations (11) and (12) differ only in scaling. Also, the  $L_2$  norms, as defined in equation (5), of the ladder states are  $\frac{1}{\beta_i}$  where  $\beta_i$  is given by equation (13). These simple properties appear to have never been mentioned in previous literature.

In order to implement the numerator of a particular transfer-function, the proper  $c$  vector must be obtained. To find the required  $c$  vector, we first need to find the states of the system. To find the states, note from figure 1 that the first state of the ladder,  $V_{r_1}$ , is an all-pole function with unity gain at DC. Hence, the numerator of the first state of the ladder is  $\mathbf{E}(0)$  where  $\mathbf{E}(s)$  is the natural mode polynomial. Using this fact together with the state equations of the orthonormal ladder system, we can write the orthonormal states

recursively as

$$F_1 = \frac{\beta_1 E(0)}{E(s)} \quad (15)$$

$$F_2 = \frac{s}{\alpha_1} F_1 \quad (16)$$

$$F_i = \left[ \frac{1}{\alpha_{i-1}} \right] (sF_{i-1} + \alpha_{i-2}F_{i-2}) \quad 3 \leq i \leq N \quad (17)$$

The proper  $c$  vector is found as the multiplying coefficients required to create the desired numerator.

We note from equations (15)-(17) that the numerators of the odd states will be even polynomials while the numerators of the even states will be odd polynomials. This fact helps to explain why an output summing amplifier which implements the  $c$  vector does not have poor sensitivity properties. Specifically, in the case of finite transmission zeros on the  $j\omega$  axis, where the transmission-zero polynomial  $P(s)$  is purely even or odd, only even or odd elements of the  $c$  vector will be non-zero. Thus, a small change in any of the non-zero  $c$  elements will result in transmission zeros which remain on the  $j\omega$  axis.

Figure 2 shows a block diagram of a general orthonormal ladder filter. The simple leap frog structure is a result of simulating a singly-terminated ladder. As shown in the block diagram, the output is obtained as a linear combination of the integrator outputs<sup>2</sup>.

Although output summing (having a  $c$  vector with more than one non-zero element) does not have poor sensitivity performance, there are situations where a circuit implementation of the  $c$  vector is difficult. An example of such a situation is the design of high frequency transconductance-C filters where a wide-band output summing network is

---

<sup>2</sup>Note that, from equation (14), the units of  $\alpha_i$  are Hz as expected. However, the units of the feed-in term is  $\sqrt{\text{Hz}}$ . This surd term is a result of forcing the states to have the same RMS value when a signal of constant spectral density in  $V/\sqrt{\text{Hz}}$  is applied at the filter input.

difficult to implement. In such a situation, it is much easier to add one more input to each of the integrators than to design a high frequency summing stage with many inputs. For these situations, feed-forward (having a  $\mathbf{b}$  vector with more than one non-zero element) can be used to create the required transmission zeros. It is important to note, however, that the feed-forward system to be described does not have an orthonormal set of  $\mathbf{F}$  functions.

In order to create a feed-forward system, an orthonormal ladder system with output summing is first obtained. The feed-forward system can be obtained by creating a new state-space system related to the orthonormal ladder system by [7]

$$\mathbf{A}_{feed} = \mathbf{A}_{ortho}^T \quad \mathbf{b}_{feed} = \mathbf{c}_{ortho} \quad \mathbf{c}_{feed} = \mathbf{b}_{ortho} \quad d_{feed} = d_{ortho} \quad (18)$$

It is easily shown from equation (2) that the two systems will have the same transfer-function. It is also not difficult to show that the following relationship holds between the intermediate-functions,  $\mathbf{F}$  and  $\mathbf{G}$ , of the orthonormal system and the feed-forward system.

$$\mathbf{F}_{feed} = \mathbf{G}_{ortho} \quad \mathbf{G}_{feed} = \mathbf{F}_{ortho} \quad (19)$$

Thus, for the feed-forward system, the intermediate set of functions  $\mathbf{G}_{feed}$  will be an orthonormal set. Since the intermediate-functions are simply interchanged, it is also easy to show from the sensitivity formulae in [3] that the feed-forward and orthonormal systems will have the same sensitivity performance with respect to system elements. Finally, although the feed-forward system does not have the  $\mathbf{F}$  functions scaled for optimum dynamic range, these functions can be  $L_2$  scaled to equal levels using the standard method of scaling.

## 4. Design Example

Consider a fifth-order elliptic lowpass transfer-function

$$T(s) = \frac{P(s)}{E(s)} = \frac{0.01321s^4 + 0.1037s^2 + 0.1739}{s^5 + 0.9287s^4 + 1.7726s^3 + 1.0557s^2 + 0.6917s + 0.1739} \quad (20)$$

The reactive elements of the singly-terminated ladder which realizes these poles can be found using partial fraction expansion[6] on the polynomial,  $E(s)$ . Applying such a procedure results in the following elements.

$$r_1 = 0.9078 \quad r_2 = 2.0205 \quad r_3 = 1.9937 \quad r_4 = 1.4606 \quad r_5 = 1.0768 \quad (21)$$

Using equation (14), the following elements of the orthonormal ladder system are obtained.

$$\alpha_1 = 0.7384 \quad \alpha_2 = 0.4982 \quad \alpha_3 = 0.5860 \quad \alpha_4 = 0.7934 \quad \alpha_5 = 0.9287 \quad (22)$$

The intermediate-functions of the orthonormal system are found using equations (15)-(17) and are

$$F_1 = \frac{0.09346}{E(s)} \quad (23)$$

$$F_2 = \frac{0.1266s}{E(s)} \quad (24)$$

$$F_3 = \frac{0.2540s^2 + 0.1385}{E(s)} \quad (25)$$

$$F_4 = \frac{0.4335s^3 + 0.3440s}{E(s)} \quad (26)$$

$$F_5 = \frac{0.5437s^4 + 0.6181s^2 + 0.1018}{E(s)} \quad (27)$$

We easily find the  $c$  vector and scalar  $d$  required to form our desired numerator to be

$$\mathbf{c}^T = [1.3163 \ 0 \ 0.3492 \ 0 \ 0.02431] \quad d = 0 \quad (28)$$

## 5. Sensitivity Performance Comparison

This section will compare the sensitivity performance of orthonormal ladder filter realizations with realizations resulting from two alternate synthesis methods. One of the alternate methods is a state-space simulation of a doubly-terminated LC ladder filter [8]. The other method is a cascade of second-order sections implemented with Tow-Thomas biquads. The finite transmission zeros of the biquads are realized using feed-forward with a resistor and a capacitor. Pole-zero pairing and cascade ordering are chosen using the rule-of-thumb in [9][10]. In order to use the analysis methods in [3], we require the cascade structure in a state-space formulation. Fortunately, a cascade of biquads design can be easily put into a state-space description if one allows a non-constant feed-back matrix. The non-constant feed-back matrix,  $\mathbf{A}(s)$  consists of two matrices,  $\mathbf{A}_1$  and  $\mathbf{A}_2$ , such that

$$\mathbf{A}(s) = \mathbf{A}_1 + s\mathbf{A}_2 \quad (29)$$

With an active-PC circuit, the  $\mathbf{A}_2$  elements are realized with capacitor feed-ins to integrators. Finally, for a fair comparison with orthonormal ladder filters,  $L_2$  dynamic range scaling was always performed on filters before comparing sensitivity or dynamic range.

Since different criteria are used to judge the filter performance in the passband and stopband, slightly different measures will be used in the two regions. However, in both bands, the multiparameter sensitivity value presented by Schoeffler [11] is used to find the standard deviation in the transfer-function for standard deviations of 1 percent of the nominal component values. The transfer-function deviation,  $\sigma|T(j\omega)|$ , is found from

$$\sigma|T(j\omega)| = 0.01 \left[ \sum_{x=a_j, b_i, c_i, \gamma_i} \left[ \frac{\partial |T(j\omega)|}{\partial x} x \right]^2 \right]^{\frac{1}{2}} \quad (30)$$

where  $\frac{\gamma_i}{s}$  represents the gain of the  $i$ 'th integrator. Formulae in [3] were used to obtain the above derivative. This deviation measure takes into account all the passive elements of an active-RC implementation.

Since transfer-function deviation is often the most critical performance measure in the passband, the passband deviation in dB,  $D(\omega)$ , is used for sensitivity performance in the passband.  $D(\omega)$  is found from  $\sigma|T(j\omega)|$  and  $|T(j\omega)|$  as

$$D(\omega) = 20\text{LOG}\left(1 + \frac{\sigma|T(j\omega)|}{|T(j\omega)|}\right) \quad (31)$$

This passband measure gives the standard deviation of the passband in dB from the ideal response for standard deviations of 1 percent of component values.

In the stopband, an expected gain curve is plotted. This stopband expected gain value,  $T_\sigma(\omega)$ , is found from

$$T_\sigma(\omega) = 20\text{LOG}[|T(j\omega)| + \sigma|T(j\omega)|] \quad (32)$$

This stopband measure allows one to easily see the expected stopband gain for standard deviations of 1 percent of component values. Note that if the passband deviation measure were used in the stopband, it would go to infinity at transmission zeros.

For dynamic range comparisons, the figure of merit  $\sum_i \|G_i\|_2^2$  will be used [3]. This figure of merit is the total output noise power obtained when uncorrelated white noise sources of unit power spectral density are applied to each of the integrator inputs. Thus, a filter with good dynamic range will have a low number for  $\sum_i \|G_i\|_2^2$ .

For the fifth-order example above, three state-space descriptions were obtained using the different design approaches. The state-space system for the ladder simulation is

$$\mathbf{A} = \begin{vmatrix} -0.4643 & -0.5823 & 0 & -0.0821 & -0.0045 \\ 0.8408 & 0 & -0.5994 & 0 & 0 \\ -0.1064 & 0.5271 & 0 & -0.4961 & -0.0272 \\ 0 & 0 & 0.6153 & 0 & -0.5892 \\ -0.0097 & 0.0479 & 0 & 0.7574 & -0.4643 \end{vmatrix} \quad \mathbf{b} = \begin{vmatrix} 0.4655 \\ 0 \\ 0.1066 \\ 0 \\ 0.0097 \end{vmatrix} \quad (34)$$

$$\mathbf{c}^T = [ 0 \ 0 \ 0 \ 0 \ 1.3620 ] \quad d = 0$$

and the state-space system for the biquad cascade is

$$\mathbf{A} = \begin{vmatrix} -0.3379 & 0 & 0 & 0 & 0 \\ -0.7709 & 0 & -0.7967 & 0 & 0 \\ (0.0922)s & 0.6491 & -0.4577 & 0 & 0 \\ 0 & 0 & 1.4464 & 0 & -1.8603 \\ 0 & 0 & (0.3191)s & 0.5348 & -0.1330 \end{vmatrix} \quad \mathbf{b} = \begin{vmatrix} 0.3297 \\ 0 \\ 0 \\ 0 \\ 0 \end{vmatrix} \quad (36)$$

$$\mathbf{c}^T = [ 0 \ 0 \ 0 \ 0 \ 1.3622 ] \quad d = 0$$

Figure 3 shows a plot of the ideal transfer-function response along with passband deviations,  $D(\omega)$ , and stopband expected gain,  $T_{\sigma}(\omega)$  curves. We see from these curves that the orthonormal ladder system has a passband performance somewhere between the performance of the ladder simulation and the biquad cascade. The stopband performance of the orthonormal ladder system is slightly worse than that of a cascade of biquads. The total output noise for the ladder, orthonormal, and cascade filters of this fifth-order example are 47,65, and 117 respectively.

An eighth-order elliptic bandpass filter example presented in [3] was also investigated. For this eighth-order example, the resulting curves are shown in figure 4. We see from these curves that the orthonormal ladder filter still performs quite well in the passband and upper stopband but is slightly worse than the other two designs in the lower stopband. The reason for the poorer sensitivity performance at DC is explained as follows. The cascade design contains two bandpass filter biquads and therefore varying any of the components will not affect the two zeros at DC. Similarly, the ladder simulation

will always have two zeros at DC because we are simulating a ladder with two zeros at DC. However, the orthonormal ladder filter creates the two DC zeros by an output summing network and thus the zeros will shift away from DC with component variations. The total output noise for the ladder, orthonormal, and cascade filter for this eighth-order example are 73, 100, and 151 respectively.

These two examples indicate that an orthonormal ladder filter has a passband sensitivity performance as least as good as a cascade of biquads (often much better) and a slightly worse stopband performance. The dynamic range performance of orthonormal ladder filters appears to fall between that obtained with LC ladder simulations and cascade designs.

## 6. Application Areas

This section will discuss what we feel are important application areas for orthonormal ladder filters other than as a general filter synthesis technique. The first application area is programmable filters. When changing a filter circuit from one transfer-function to another, it is important that the performance of the circuit not be severely degraded. Since we have shown that the orthonormal ladder structure is inherently scaled for optimum dynamic range, the circuit's elements can be changed to new values while maintaining the circuit's good dynamic range.

Similar to programmable filters is the field of adaptive filters. In this case, the filter's parameters are dynamically changed to minimize some error criteria. If one has an algorithm to adapt the poles of the system then, as above, an orthonormal filter can be adapted and maintain good dynamic range. However, there is another property of orthonormal ladder filters which lends itself well to adaptive filters. The fact that the

integrator outputs are all orthogonal with white noise at the input is quite important. It is shown in [12] that with an adaptive linear combiner, adaptation is much faster if all the inputs to the linear combiner are orthogonal. Thus, if the  $\mathbf{A}$  and  $\mathbf{b}$  elements remain fixed and the  $\mathbf{c}$  vector of the state-space system is used as a linear combiner, the adaptation process converges quickly. One reason to consider analog adaptive filters is to process signals with much higher frequency contents than is now possible with digital filters [13].

## 7. Conclusions

We have presented a new filter structure called orthonormal ladder filters. These filters are easy to synthesize through the use of singly-terminated LC ladders. As well, orthonormal ladder filters are automatically  $L_2$  scaled for optimum dynamic range by the very nature of their structure. Also inherent in their structure is the fact that the integrator outputs are all orthogonal when the input is excited by white noise. We have also shown that orthonormal ladder filters can realize any stable transfer-function and have a performance comparable to a cascade of biquads. We feel that orthonormal ladder filters should be useful as a general design method and may be useful in the implementation of programmable or adaptive filters.

It was also shown that a singly-terminated LC ladder driven through its resistor has orthogonal states. As well, the  $L_2$  norm of the ladder states were shown to have a simple relationship to the elements of the ladder.

## References

[ 1] H.J. Orchard, "Inductorless Filters", Electron Lett., vol. 2, pp. 224-225, June 1966

[2] R.A. Roberts and C.T. Mullis, *Digital Signal Processing*, Reading, Mass.: Addison-

Wesley Publishing, 1987.

[3] W.M. Snelgrove and A.S. Sedra, "Synthesis and Analysis of State-Space Active Filters Using Intermediate Transfer Functions", *IEEE Trans. on Circuits and Systems*, vol. CAS-33, pp. 287-301, March 1986.

[4] R.W. Brockett, *Finite Dimensional Linear Systems*, New York, N.Y.: John Wiley and Sons, 1970.

[5] Chi-Tsong Chen, *Linear System Theory and Design*, New York, N.Y.: Holt Rinehart and Winston, 1984.

[6] D.S. Humpherys, *The Analysis, Design, and Synthesis of Electrical Filters* Englewood Cliffs, N.J.: Prentice-Hall, Inc., 1970.

[7] L.B. Jackson, "On the Interaction of Roundoff Noise and Dynamic Range in Digital Filters", *Bell Syst. Tech. J.*, vol. 49, pp. 159-184, 1970.

[8] D.A. Johns and A.S. Sedra, "State-Space Simulation of LC Ladder Filter", *IEEE Trans. on Circuits and Systems*, vol. CAS-34, pp. 986-988, August 1987.

[9] A.S. Sedra and P.O. Brackett, *Filter Theory and Design: Active and Passive*. Portland, OR: Matrix, 1978.

[10] G.S. Moschytz, *Linear Integrated Networks: Design*. New York: Van Nostrand Reinhold, 1975.

[11] J.D. Schoeffler, "The Synthesis of Minimum Sensitivity Networks", *IEEE Trans.*

*Circuit Theory*, vol. CT-1 1, pp. 271-276, 1964.

[12] B. **Widrow** and S.D. Stearns, *Adaptive Signal Processing*, Englewood Cliffs, N.J.: Prentice-Hall, Inc., 1985

[13] H. Lev-Ari, J.M. Cioffi, and T. Kailath, "Continuous-time Least Squares Fast Transversal Filters", *Proc. IEEE Int. Conf. Acoust., Speech and Signal Processing*, pp. 415-418, Dallas, Texas, April 1987.

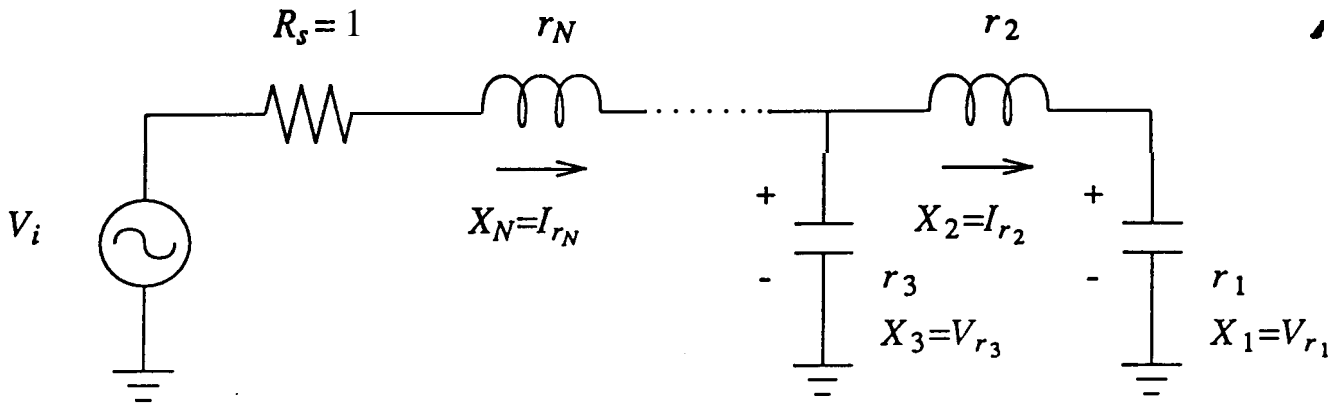


Figure 1: A singly terminated ladder and its states

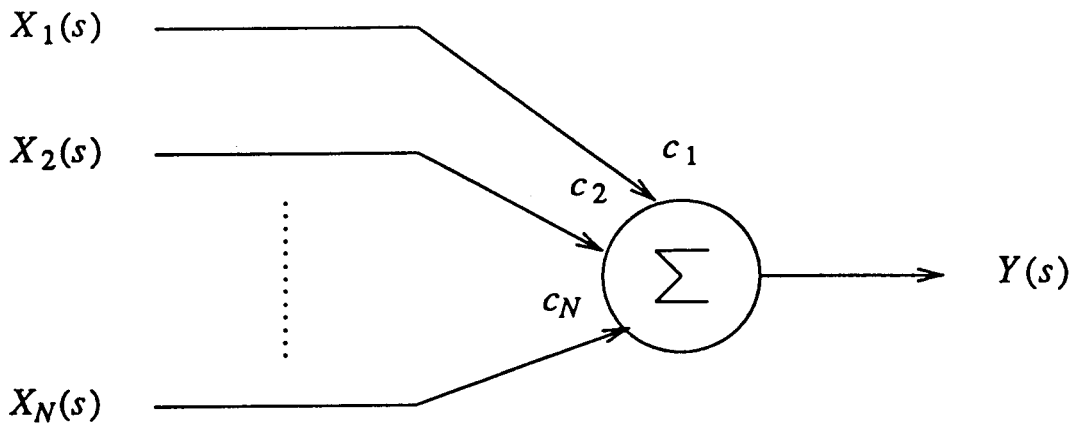
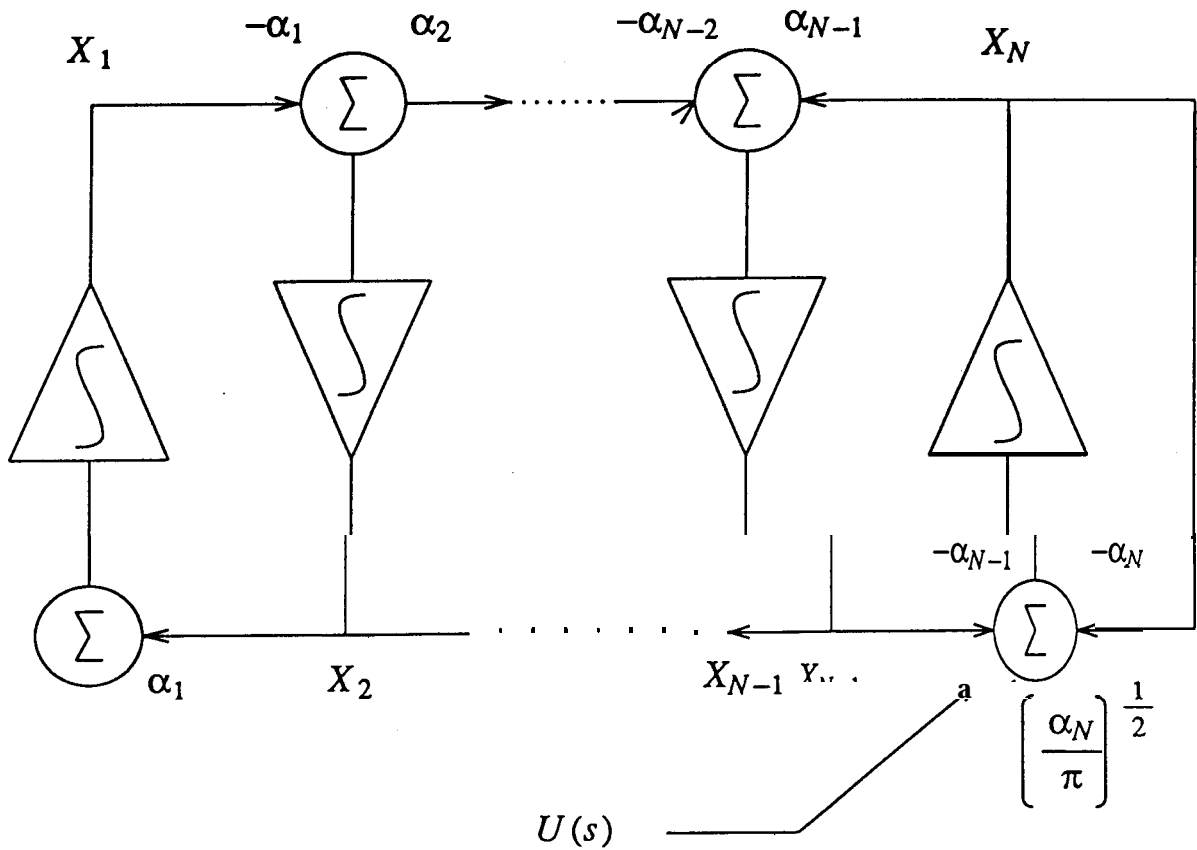


Figure 2: Block diagram of an orthonormal ladder filter

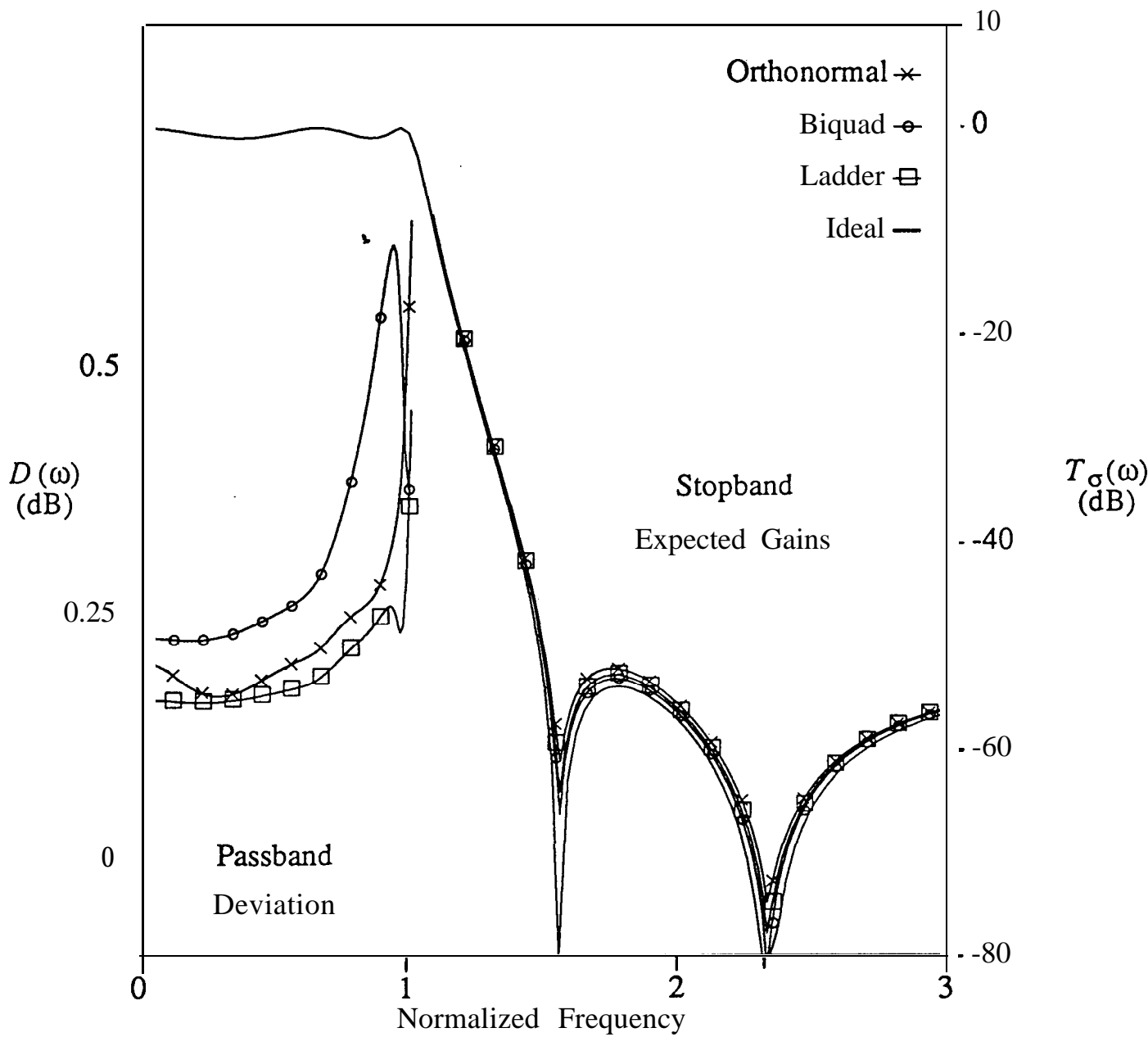


Figure 3: Fifth-order **example**: Sensitivity curves for standard deviations of 1% of component values

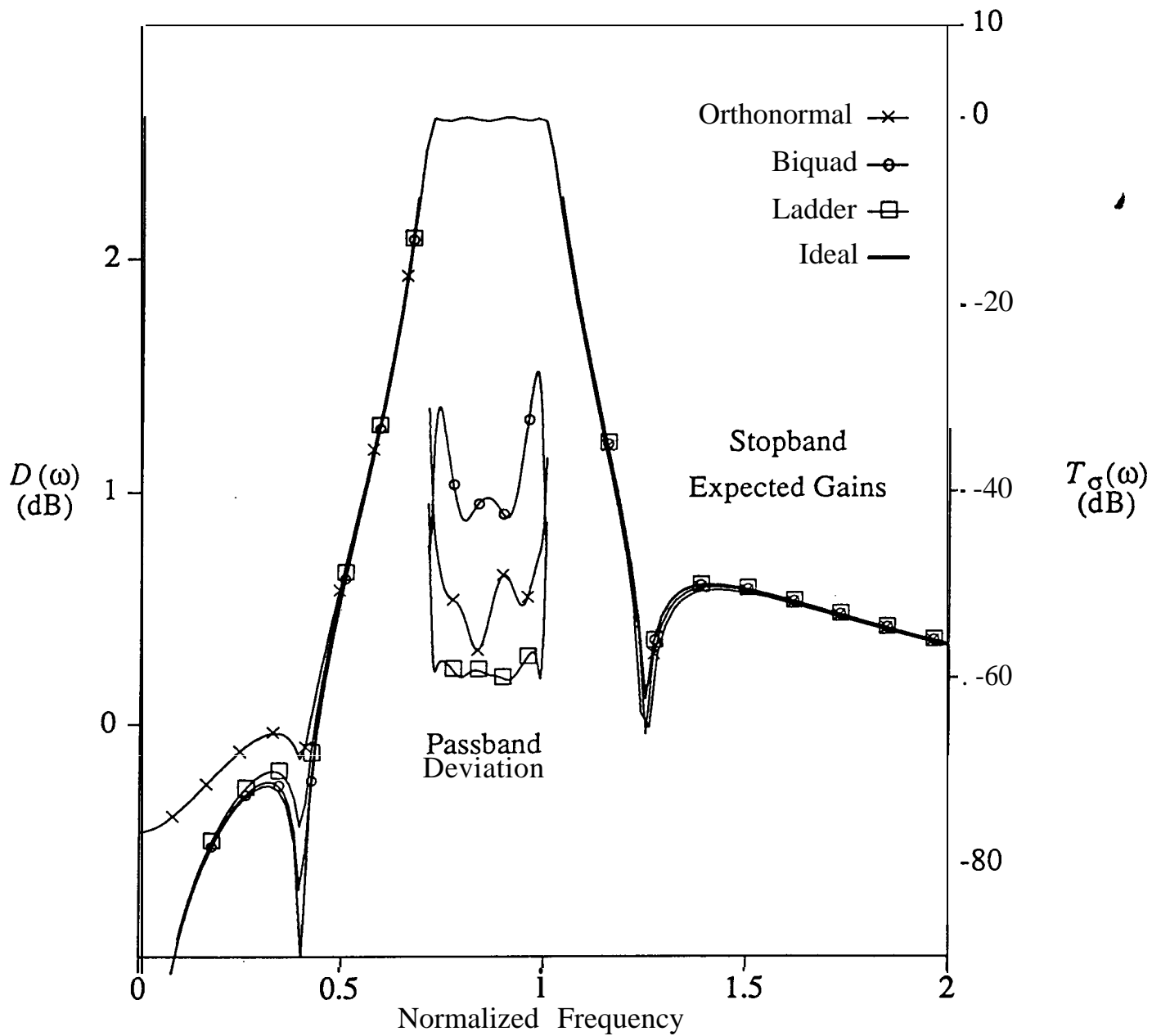


Figure 4: Eighth-order example: Sensitivity curves for standard deviations of 1% of component values